Available online at www.sciencedirect.com
ScienceDirect
Polymer Testing 26 (2007) 361–368
POLYMER TESTING
www.elsevier.com/locate/polytest

Material Characterisation

Rapid manufacturing of PA/HDPE blend specimens by selective laser sintering: Microstructural characterization

G.V. Salmoria[a,*], J.L. Leite[a], C.H. Ahrens[a], A. Lago[b], A.T.N. Pires[c]

[a]*CIMJECT, Departamento de Engenharia Mecânica, Universidade Federal de Santa Catarina, UFSC 88040-900 Florianópolis, SC, Brazil*
[b]*LABMAT, Departamento de Engenharia Mecânica, Universidade Federal de Santa Catarina UFSC 88040-900 Florianópolis, SC, Brazil*
[c]*POLIMAT, Departamento de Química, Universidade Federal de Santa Catarina UFSC, 88040-900 Florianópolis, SC, Brazil*

Received 23 October 2006; accepted 4 December 2006

Abstract

The structure and properties of parts made by selective laser sintering (SLS) depend on the process parameters and the characteristics of the powder material to be processed. The use of polymeric blends can increase the range of structures and properties of SLS parts. This study investigates the processing of blends of polyamide (PA2200) and high-density polyethylene (HDPE) by SLS using a CO_2 laser. Powder properties of undiluted polymers, mixture composition, processing parameters and their influence on the microstructure of the specimens manufactured, were evaluated. PA2200 showed higher absorption of laser energy than HDPE during the sintering of blend specimens, with subsequent thermal energy transfer to the melting of the HDPE phase. The microstructures of PA2200/HDPE blend specimens were heterogeneous with co-continuous and disperse phases depending on the quantity of HDPE. The porosity and crystallinity also changed as a function of the component proportions. These results suggest that it is feasible to manufacture blend parts using SLS, with control over the structure and properties being achieved through selecting the polymer properties (laser absorption and melt flow), powder characteristics (form and size distribution) and the optimum process parameters according to the blend composition.

Keywords: Selective laser sintering; Microstructure; PA/HDPE blends

1. Introduction

Selective laser sintering (SLS) is a rapid prototyping (RP) or solid free-form (SFF) manufacturing technology, in which a tri-dimensional solid object is built, layer-by-layer, through the sintering of powder materials using an infrared laser beam. The SLS process offers advantages such as high geometrical freedom and dimensional precision, allowing the manufacture of parts with well-defined details [1–3]. It also offers high-process flexibility with regard to the materials that can be processed. Due to these characteristics, SLS is commonly used in the manufacture of prototypes and parts in different fields including the electronic, mechanical and biomedical areas [1–12].

The structure and properties of the parts to be manufactured by selective laser sintering should be considered according to their application. The level

*Corresponding author.
E-mail address: gsalmoria@cimject.ufsc.br (G.V. Salmoria).

0142-9418/$ - see front matter © 2007 Elsevier Ltd. All rights reserved.
doi:10.1016/j.polymertesting.2006.12.002

of control over the microstructure of the SLS parts depends on the process parameters, particularly the powder properties [3–6], since these can influence other parameters. For example, particle shape and size distribution influences the powder packing density, while the melting flow behavior and the thermal stability define the laser power and scan speed [1,3,4].

The use of polymeric materials in the SLS process offers some advantages over metallic and ceramic materials, which are related to the low processing temperatures, melting flow control and high corrosion resistance. However, the variety of commercial polymeric materials available for the SLS process is restricted and this reduces the options available during material selection for the manufacturing of particular parts [4–12]. The use of non-commercially available polymers and mixtures of polymers can increase the range of properties of the SLS parts [10–12].

Polymeric blends offer an alternative means to obtain SLS parts with specific structure and properties, permitting the development of new applications. Most polymeric blends are multiphase systems and, therefore, their properties largely depend on their microstructure. This study investigated the microstructure of polyamide (PA2200) and high-density polyethylene (HDPE) blend specimens manufactured by SLS. Powder material properties, mixture composition, processing conditions and their influence on the microstructure of the specimens are discussed.

2. Experimental

2.1. Materials

The polymeric powders used in this study were commercial polyamide PA2200 (EOSINT) and high-density polyethylene HD7555 (Ipiranga S.A.) with average particle sizes of 60 and 100 μm, respectively. The HDPE particles were pre-treated by heating (120–125 °C) in glycerol under mechanical stirring for 1 h to improve the particle regularity.

Table 1
Melt flow index of PA2200 and HDPE at different temperatures

	Temperature (°C)	MFI (g/10 min)
PA2200	200	2.38
	230	17.9
	260	41.8
HDPE	140	0.79
	170	2.65
	200	4.27

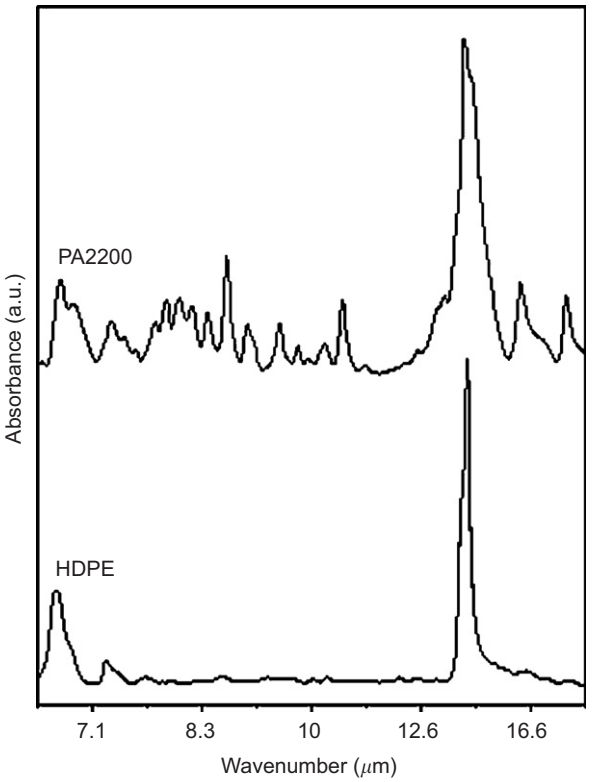

Fig. 1. Infrared spectra for PA2200 and HDPE.

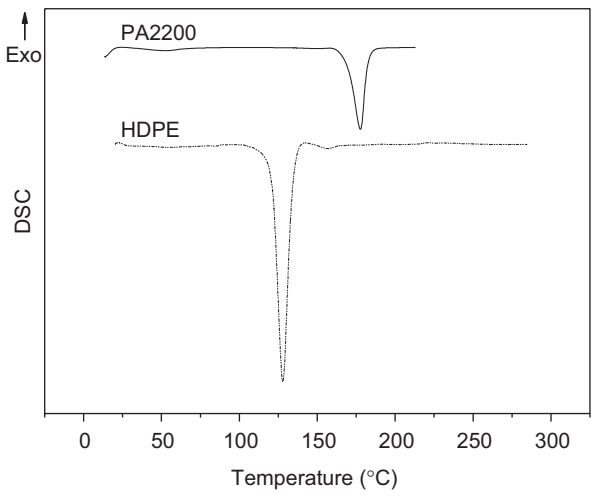

Fig. 2. DSC curves for PA2200 and HDPE powder.

2.2. Selective laser sintering of specimens

The specimens (dimension: $10 \times 5 \times 3$ mm) of undiluted polymers and mixtures of PA2200 and HDPE powders of 80/20, 50/50 and 20/80 (w/w) were processed by SLS using a 20 W RF-excited CO_2 laser (wavelength: 10.6 μm; laser beam diameter: 250 μm). The processing parameters were: layer thickness 150 μm, laser scan speed 80 mm/s and chamber temperature 60 °C. The laser power was 3, 12 and 6 W for the PA2200, HDPE and PA2200/HDPE blends, respectively.

2.3. Infrared spectroscopy, differential scanning calorimetry and melt flow measurements

Infrared spectra of the polymers were obtained using a 16 PC Perkin-Elmer spectrophotometer,

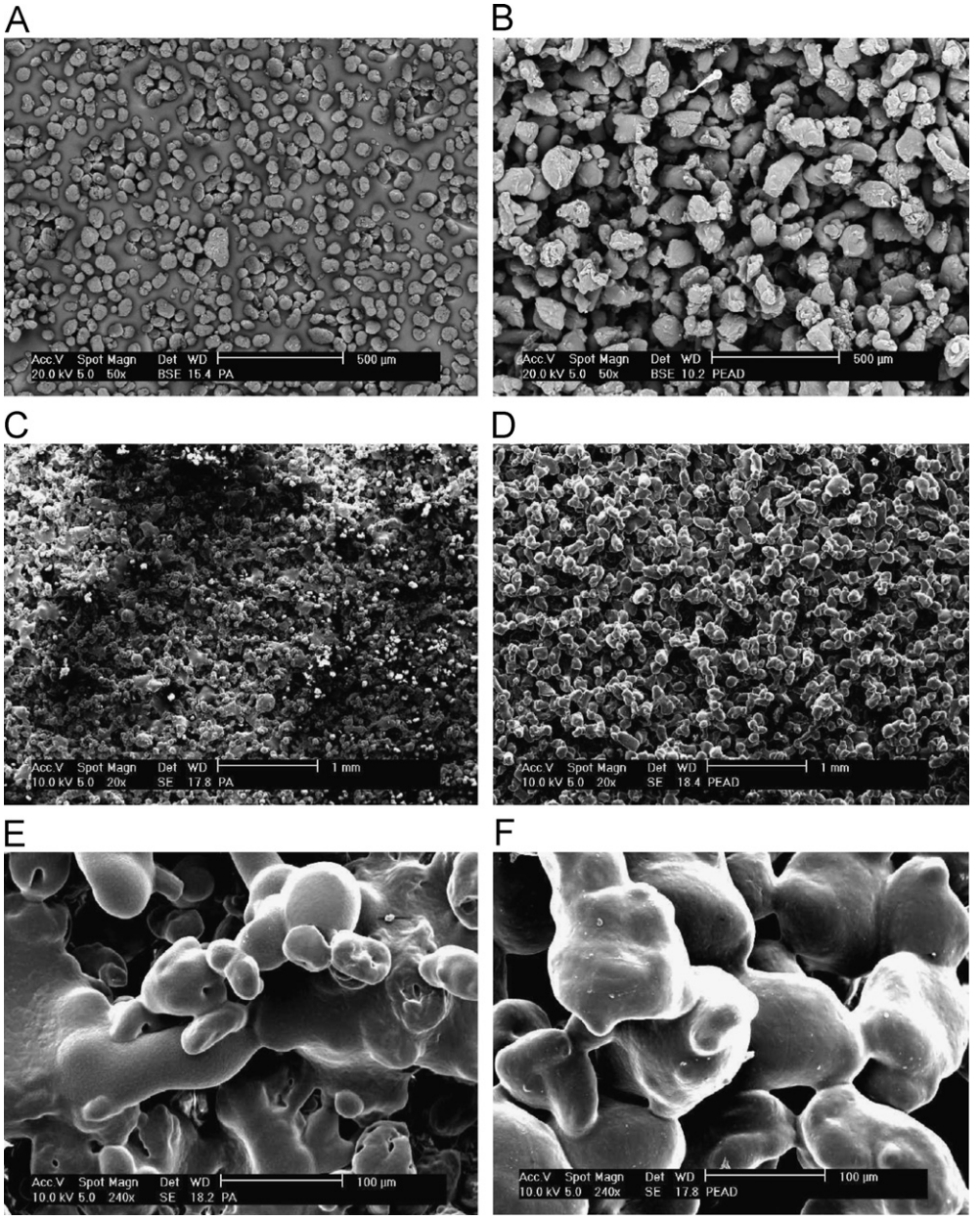

Fig. 3. Micrographs for: (A) PA2200 powder, (C) and (E) PA2200 specimen 20× and 240× magnification, respectively, (B) HDPE powder, (D) and (F) HDPE specimen 20× and 240× magnification, respectively.

performing 20 scans at a resolution of 4 cm^{-1} using KBr plates, in order to evaluate polymer absorbance at the CO_2 laser wavelength.

Differential scanning calorimetry (DSC) curves were obtained using a differential scanning calorimeter (Shimatzu 50) from 25 to 300 °C at a heating rate of 10 °C min^{-1}. The average sample size was 5 mg and the nitrogen flow rate was 25 cm^3 min^{-1}.

The melt flow index (MFI) was determined at different temperatures (Table 1) and moderated strain rate using 1.0 kg of static mass in a T.Q.-CEAST equipment according to ASTM 1238D.

2.4. Scanning electron microscopy and X-ray diffraction

The polymer powders and specimens were inspected using a Philips XL30 scanning electron microscope (SEM) in order to investigate their particle aspects, microstructures and cryogenic fracture topographies. SEM-EDX analysis was performed on samples to examine the microstructure features. The specimens were coated with gold in a Bal-Tec Sputter Coater SCD005.

The X-ray diffraction measurements were performed using a Philips PW1150 vertical diffractometer. The Cu–K_α nickel filtered radiation was detected in the range of 6–50°. These analyses were used to control the microstructure of the specimens.

3. Results and discussion

Fig. 1 shows the infrared spectra of PA2200 and HDPE from 6.0 to 25.0 μm. At 10.6 μm is possible to observe an absorption band in the PA2200 spectrum, corresponding to the vibration of amide groups, and the absence of an absorption band at this wavelength for the HDPE spectrum. The absence of absorption at 10.6 μm can be explained by the greater amount of laser power needed to process HDPE (experimental section), even though it has a lower melting temperature than PA2200, as revealed by the DSC curves (Fig. 2). The melting temperatures and enthalpies obtained for PA2200 and HDPE were 178 °C and 46 J g^{-1} and 128 °C and 124 J g^{-1}, respectively.

PA2200 and HDPE with average sizes of 60 and 100 μm, respectively, had irregular particle shapes as shown in the powder micrographs (Figs. 3A and B). The surface of pure PA2200 and HDPE sintered specimens (Figs. 3C and D) had homogeneous distributions of interconnected pores with average size being related to the particle size and shape of the original powder. With the processing parameters used in the SLS, the PA2200 and HDPE specimens showed a higher sintering degree, with particles united by extensive neck formations, as can be observed in the higher magnification micrographs shown in Figs. 3E and F.

Fig. 4 shows the X-ray diffractograms for the PA2200 and HDPE powders and sintered specimens.

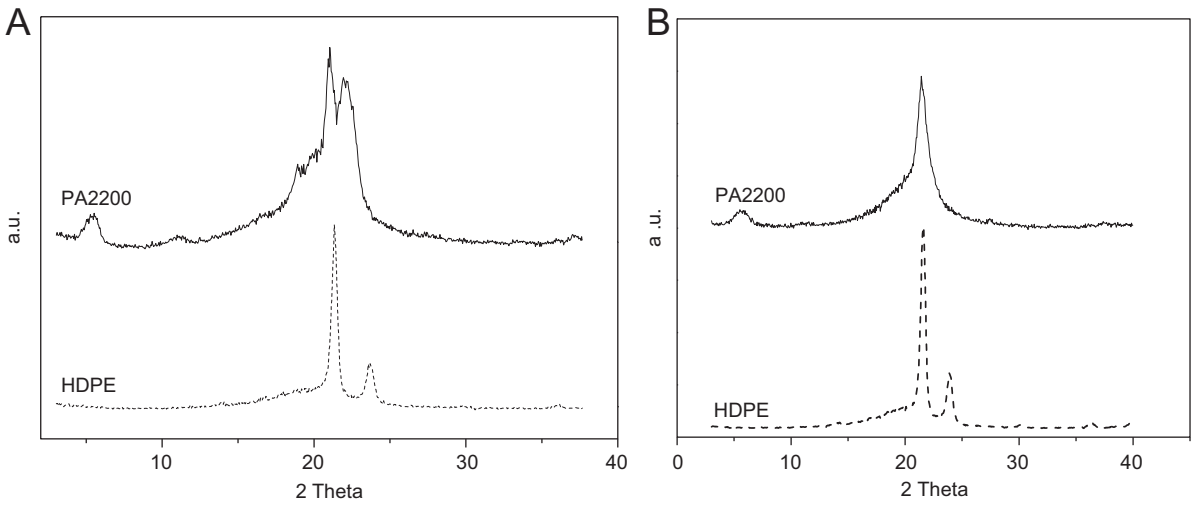

Fig. 4. X-ray diffractograms for PA2200 and HDPE powder (A) and specimens (B).

Polyamides can crystallize into more than one crystal structure with different chain folding patterns, which influence the mechanical properties. The α phase (monoclinic or triclinic) is the usual phase found for polyamides with a low number of methylene units. The γ phase (pseudohexagonal) is found in polyamides with a larger number of methylene units due to the improved van der Waals interactions between methylene groups [13]. The X-ray diffractogram given in Fig. 4A shows that the PA2200 powder before sintering gave reflection peaks 100 and 010/110 at 2θ of 20° and 24° relating to the α phase and 21° relating to the γ phase [13,14]. The PA2200 sintered specimen gave only a reflection peak at 21° relating to the γ phase (Fig. 4B), due to fast thermal exchanges involved in the laser powder sintering. The γ phase is not thermodynamically stable, being predominant under fast cooling conditions [13]. The X-ray

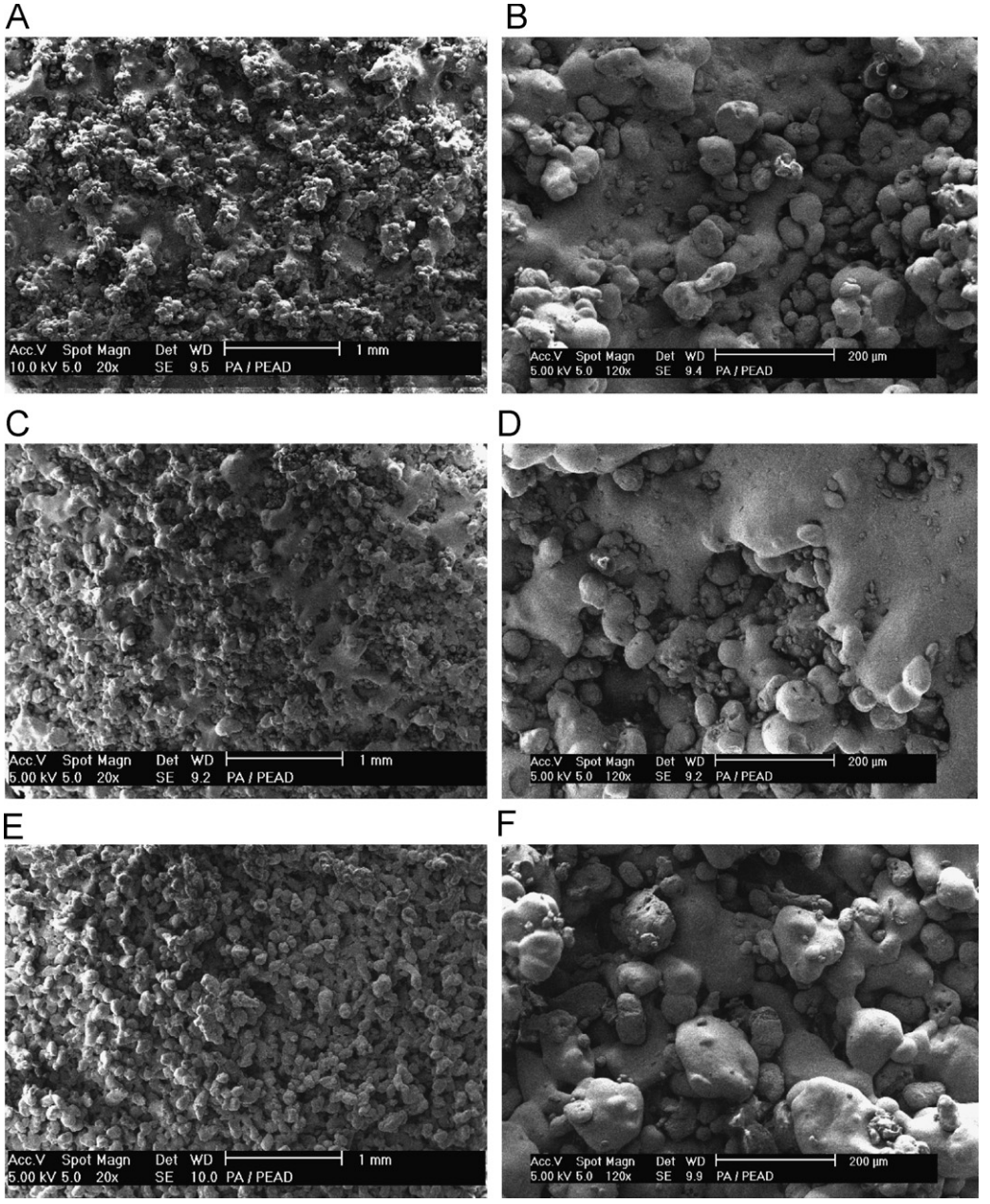

Fig. 5. Surface micrographs for PA2200/HDPE specimens: (A) and (B) 80/20 w/w composition, (C) and (D) 50/50 w/w composition and (E) and (F) 20/80 w/w composition at 20 × and 240 × magnification, respectively.

diffractogram for the HDPE powder in Fig. 4A gave peaks at 2θ of 22° and 24°, related to the reflection peaks 110 and 200 of the most common phase of polyethylene (orthorhombic phase) [15]. The HDPE sintered specimen also gave crystalline peaks relating to the orthorhombic phase (Fig. 4B).

After the evaluation of the microstructure characteristics of the pure specimens, the specimens of PA2200 and HDPE blends in different compositions were analyzed. The micrographs of the specimen surfaces of the PA2200/HDPE blends in compositions of 80/20, 50/50 and 20/80 (w/w) are shown in Fig. 5. In the microstructure of the PA2200/HDPE specimen with a 80/20 composition, the formation of a PA2200 and HDPE co-continuous phase occurred, with particles of PA2200 adhered to it. The specimen showed pores with diameters $<200\,\mu m$.

The surface micrographs of the PA2200/HDPE specimen in a 50/50 composition showed the formation of a large co-continuous HDPE phase and some particles of PA2200 adhered to the matrix, as confirmed by the presence of oxygen from amide groups in the EDX analysis of the particles (Fig. 6). The surface micrographs of the PA2200/HDPE specimen in a 50/50 composition showed lower porosity than the specimen in a 80/20 composition, due to the quantity of co-continuous phase HDPE, since PA2200 has a higher laser absorption and melting temperature than HDPE. The mechanism of microstructure formation during the laser sintering is: (i) PA2200 absorbs the laser energy and transfers it to HDPE particle melting and (ii) HDPE has a significant melt flow compared to PA2200 under the process conditions, resulting in HDPE particle coalescence and co-continuous phase consolidation. It can be estimated by MFI values at 200 °C described in Table 1.

In the surface micrographs of the PA2200/HDPE specimen in a 20/80 composition it was possible to observe a microstructure with high porosity, as in the microstructure of the pure HDPE specimen (Fig. 3). The HDPE phase has a sintered matrix pattern, which differs from the microstructure of other blends (80/20 and 50/50 composition), due to the low laser energy absorption shown by this blend composition (80 wt% HDPE). Some particles of PA2200 are dispersed in the HDPE matrix.

The fractured surface of the 80/20 PA2200\HDPE specimen showed microstructure features indicating the coalescence of PA2200 and HDPE particles forming co-continuous phases (Figs. 7A and B). The existence of PA2200 domains encapsulated into regions of HDPE coalescence demonstrated the low interaction between the PA2200 and HDPE phases in the mixture, as expected. Polymers with different polarity, such as PA2200 and HDPE, show low attractive force and immiscibility. The 50\50 PA2200\HDPE specimen showed dense areas due to coalescence of the HDPE as observed in the

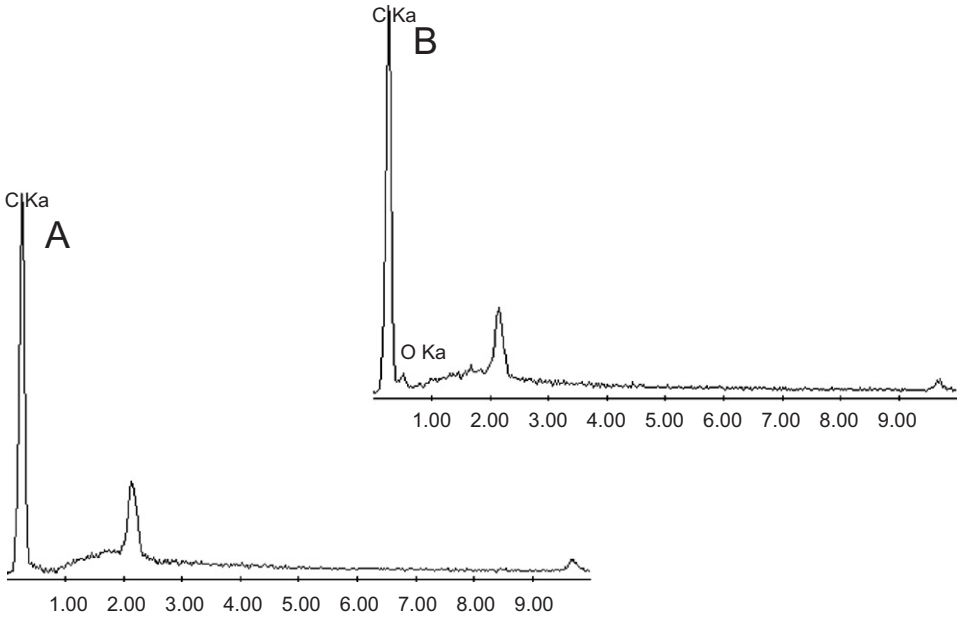

Fig. 6. EDX analysis of the continuous phase (A) and particles (B) of PA2200/HDPE 50/50 specimen.

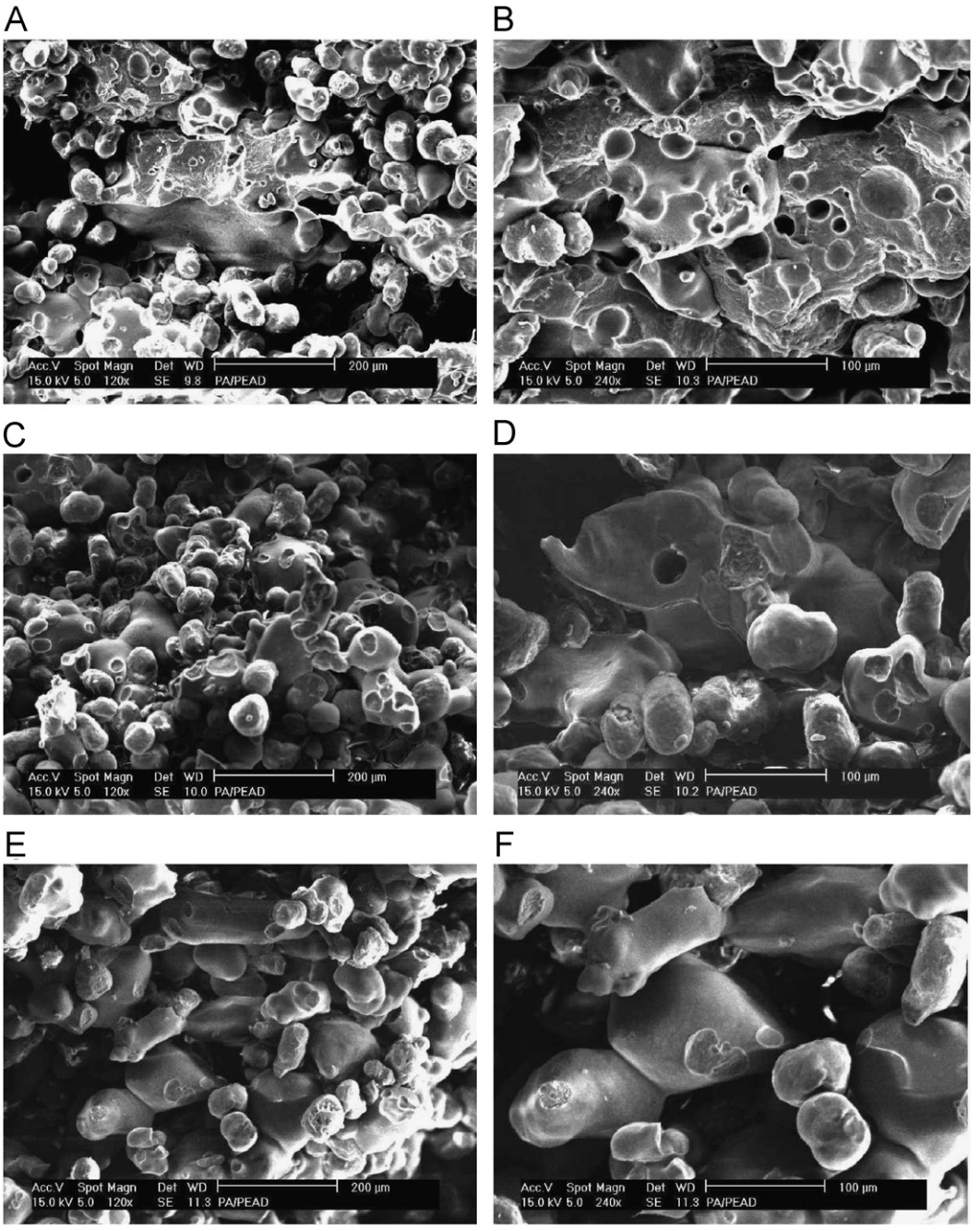

Fig. 7. Cryogenic fracture micrographs of PA2200/HDPE specimens: (A) and (B) 80/20 w/w composition, (C) and (D) 50/50 w/w composition, and (E) and (F) 20/80 w/w composition at 20 × and 240 × magnification, respectively.

surface analysis (Figs. 5C and 5D). However, the 20\80 PA2200\HDPE specimens showed particle union through neck formation and coalescence, which forms a sintered HDPE matrix with pores. This porous microstructure is formed under a moderated viscous flow and heating rate due to the lower laser energy absorption.

The X-ray diffractograms (Fig. 8) showed that PA2200\HDPE blend specimens (80/20, 50/50 and 20/80) give crystalline peaks relating to the PA2200 γ phase and orthorhombic HDPE as the sintered pure materials. The peak intensities were proportional to the blend composition. The presence of the PA2200 γ phase is due to fast thermal exchange

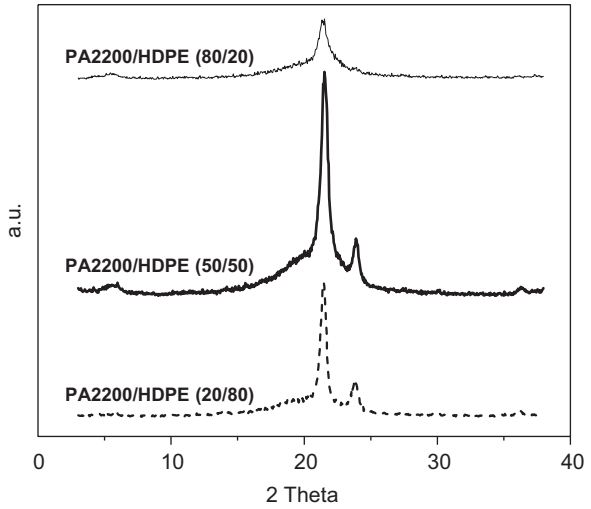

Fig. 8. X-ray diffractograms of PA2200\HDPE specimens in compositions of 80/20, 50/50 and 20/80 w/w.

involved in selective laser sintering under these conditions. The X-ray diffractogram of PA2200/HDPE 50/50 seems to give an amorphous halo, which may be related to the thermal exchanges between PA2200 and HDPE during the blend microstructure formation.

4. Conclusions

PA2200/HDPE blends prepared by SLS show the formation of semi-crystalline microstructures with co-continuous phases and porosities, which are dependent on the HDPE content. The PA2200 has higher laser absorption and melting temperature than HDPE. PA2200 absorbs the majority of the laser energy and transfers it to HDPE particles, resulting in HDPE particle coalescence and co-continuous phase consolidation. The mechanism of blend microstructure formation depends on the HDPE viscous flow during the laser sintering. The X-ray diffraction analysis showed that PA2200\HDPE blends prepared by SLS give crystalline peaks relating to the PA2200 γ phase and orthorhombic HDPE. The presence of the PA2200 γ phase in blends is due to the fast thermal exchange involved in the blend microstructure formation.

The manufacturing of blends using a selective laser sintering process demonstrated that it is possible to prepare PA2200/HDPE blends with controlled structures and properties selecting the polymer powder characteristics, such as particle size, laser absorption and melting flow behavior, and adjusting the process parameters according to the blend composition. The selective laser sintering of polymer blends permits the preparation of functional components and the development of new applications for rapid manufacturing by SLS technology.

Acknowledgments

The authors would like to thank FAPESC, CAPES, CNPq and FINEP for the financial support.

References

[1] P.F. Jacobs, Rapid Prototyping and Manufacturing: Fundamentals of Stereolithography, Society of Manufacturing Engineers, Dearborn, Michigam, USA, 1993.
[2] P.F. Jacob, From Rapid Prototyping to Rapid Tooling, ASME, New York, 1999.
[3] D.M. Bourell, H.L. Marcus, J.W. Barlow, J.J. Beaman, Selective laser sintering of metal and ceramics, Int. J. Powder Metall. 28 (1992) 369–382.
[4] K.H. Low, K.F. Leong, C.K. Chua, Z.H. Du, C.M. Cheah, Characterization of SLS parts for drug delivery, Rapid Prototyping J. 7 (2001) 262–267.
[5] T.H.C. Childs, M. Berzins, G.R. Ryder, A. Tontowi, Selective laser sintering of an amorphous polymer–simulations and experiments, Proc. Inst. Mech. Eng. 213 (1999) 333–349.
[6] H.C.H. Ho, I. Gibson, W.L. Cheung, J. Mater. Process. Technol. 89 (1999) 204–210.
[7] H.C.H. Ho, W.L. Cheung, I. Gibson, Rapid Prototyping 8 (2002) 233–242.
[8] EOSINT, Plastic laser-sintering for direct manufacturing. EOS GmgH, Technical Data. Bimingham, UK, 2002. Polyamide PA 2200 for EOSINT, Material Data Sheet.
[9] DTM, SLS process and DTM's DuraForm PA, Material Data Sheet. http://www.dtm-corp.com/home.htm.
[10] J. Kim, T.S. Creasy, Selective laser sintering characteristics of nylon 6/clay-reinforced nanocomposite, Polym. Test. 23 (2004) 629–636.
[11] K.H. Tan, C.K. Tha, K.F. Leong, C.M. Heah, P. Cheang, M.S. Abu, S.W. Cha, Biomaterials 24 (2003) 3115–3123.
[12] H. Zheng, J. Zhang, S. Lu, G. Wang, Z. Xu, Mater. Lett. 60 (2006) 1219–1223.
[13] R. Androsh, M. Stolp, H.J. Radusch, Simultaneous X-ray diffraction and differential thermal analysis of polymers, Thermochim. Acta 271 (1996) 1–8.
[14] E.D.T. Atkins, M.J. Hill, K. Veluraja, Structural and morphological investigation of nylon 8 chain-folded lamellar crystals, Polymer 36 (1995) 35–42.
[15] M. Mihailova, M. Kresteva, N. Aivazova, V. Krestev, E. Nedkov, X-ray investigation of polypropylene and poly (ethylene-co-vinyl acetate) blends irradiated with fast electrons, Radiat. Phys. Chem. 56 (1999) 581–589.